SUPPRESSION DYNAMICS OF A BOUNDARY-LAYER DIFFUSION FLAME

Ramagopal Ananth, Chuka C. Ndubizu, P.A. Tatem, Gopal Patnaik, and K. Kailasanath
Naval Research Laboratory

ABSTRACT

Flame stability, suppression, and extinction phenomena are intrinsically time dependent. Solutions are obtained for unsteady, full Navier-Stokes equations using Barely Implicit Correction to Flux Corrected Transport (BIC-FCT) algorithms for a boundary-layer diffusion flame formed over a flat porous plate, through which a fuel gas is injected uniformly. The solutions include calculation of surface temperature and composition as functions of time and position along the entire plate by an iterative method. Simulations were performed for dry air, air with steam, and air with very small water droplets to describe the effects of oxygen dilution, specific heat, and latent heat absorption at different times during the development of the flame. At steady state, without the suppressant, the model predictions for temperature and axial velocity profiles are in good agreement with the existing experimental data.

INTRODUCTION

Water mist is a leading candidate as an alternative to Halon 1301 for suppressing fires on ships. It is non-toxic, less corrosive, has zero ozone depletion potential (ODP) and does not produce hazardous chemicals such as hydrogen fluoride. However, unlike the gaseous agents that can diffuse to the fire, water droplets rely mainly on the fluid dynamics of the surrounding gas to be transported to the fire as discussed by Tatem et al. [1]. Solid surfaces naturally form boundary layers due to no-slip at the surface. Also the solid pyrolysis ejects fuel gas from the surface in the direction perpendicular to the flow of oxidizer (air). Therefore, the flame dynamics is fundamentally altered by the solid surface, which can significantly impact the effectiveness of the droplets.

Future ships, with increased automation, must rely on fixed water mist systems rather than handheld systems, in a wide range of spaces containing solid materials. Development work on water mist systems has been conducted by Mawhinney et al. **[2]** on large-scale fires. However, large-scale tests are scenario specific, and tests must be conducted with limited scope since they are expensive. The tests are too expensive to study the effects of more than a few parameters. Furthermore, the data often contain conflicting effects of various parameters and pose complexities in drawing general conclusions. Therefore, fundamental theories and numerical models are needed to gain insights into the effects of various parameters, such as, droplet number density, size, and velocity, orientation of the solid surface, air velocity, fuel type (charring vs. non-charring).

In this work, we will present a numerical model for suppression of a boundary layer diffusion flame formed over a porous plate through which a fuel gas is injected uniformly. Unlike a PMMA surface, the porous plate burner provides a well-defined boundary unencumbered by the complex phenomena, which occur in the solid phase. It allows definitive validation of the base case model, without any suppressant, against existing experimental data. We will show that the base case model predictions for steady state temperature and axial velocity are in good agreement with the experiments. We will introduce suppressant into the air flow and discuss transient solutions of full Navier-Stokes equations. We will describe flame suppression by water vapor and very small water droplets from the time of ignition to extinction for the first time. We will discuss the effects of oxygen dilution, high specific heat, and latent heat absorption. The solutions given here are valid from the leading edge to far downstream of the porous plate. They include the Defour effects and the effects of variable properties due to variation in both the temperature and composition.

There are very few theoretical studies performed on water mist interactions with flames. K. Prasad et al. **[3]** studied water mist suppression of a diffusion flame formed between two gas jets. In this co-flow

configuration, both the fuel and air jets flow out of a burner parallel to one another. Water mist is introduced with the air jet and is entrained into the flame, where the droplets evaporate to form water vapor. They predicted increased suppression in temperature with decreased droplet diameter and increased number density, and showed good agreement with the experimental data. They also studied liquid pool flame [4] in co-flow configuration and showed that the orientation of droplet injection with respect to the jets has significant effect on the degree of suppression. Lentati and Chelliah [5] considered counter-flow configuration, where the two jets oppose one another. They predicted as high as 10 times greater suppression in temperature than that observed in the co-flow studies at a fixed concentration of the mist. This appears to be due to difference in strain rates of about 50/sec and 400/sec in co-flow and counter-flow studies respectively. Therefore, configuration and velocity of air can significantly change the degree of suppression.

Flame suppression and extinction are intrinsically time-dependent phenomena. Most existing theories of boundary layer flames do not consider suppression and make boundary layer approximations, which are not valid near the leading edge of the flame [6,7,8]. Mao et al. [9] and Kodama et al. [10] obtained steady-state solutions without the boundary layer approximations, and studied the effects of oxygen dilution by nitrogen on flame extinction length (i.e., the displacement of the leading edge of the flame). Chen and Tien [11], and C. DiBlasi [12] considered flame attachment and flame spread, respectively, but did not consider the effects of a suppressant.

ANALYSIS

We consider air flow (60.0 cm/sec) past a solid surface, which consists of a leading non-porous plate (2.5 cm), followed by a porous plate (7 cm), followed by a non-porous plate (10 cm). The geometry is chosen to match the experimental setup of Ramachandra and Raghunandan [8]. The leading plate establishes the no-slip condition prior to the flame. n-Pentane gas is injected at a uniform and fixed rate (0.3 cm/sec) through the porous plate. The gases are ignited near the leading edge of the porous plate by adding external energy for a short period of time. The suppressant is added to the air stream prior to ignition at a fixed concentration. The flame dynamics is described by the full, unsteady, Navier-Stokes and energy equations with the following sink terms

$$Q_{chem} = \Delta H_c W_k \quad (1)$$

$$Q_{evap} = m_{evap} L \quad (2)$$

where, Q_{chem} (or DEDtrxn) is the heat release rate per unit volume, ΔH_c is the beat of combustion, W_k is the reaction rate for the fuel. The term $Q_{...}$ is the rate of absorption of latent heat per unit volume due to the evaporation of water droplets, and L is the latent heat of evaporation of water. The water droplets are assumed to be very small and evaporate at very high rate when the local gas temperature is above 100°C irrespective of the droplet size. Therefore, the simulations capture the latent heat effects associated with ideal droplets, and m_{evap} is set to an arbitrarily high value; increasing its value further does not affect the results significantly.

Solutions are obtained using Barely Implicit Correction to Flux Corrected Transport (BIC-FCT) algorithms with time step splitting [13]. The smallest (0.2 x 0.2 mm) cells are placed near the leading edge of the porous plate and are stretched in both directions on 150 x 200 grid. A single step combustion kinetics [14] for *n*-pentane is used and is integrated using Bulirsch-Stoer method with Rhomberg interpolation. The transport properties and specific heats are evaluated as functions of temperature and composition based on the kinetic theory of gases and polynomial expressions for enthalpy, respectively.

The species concentrations along the porous surface are determined by the mass flux balances for fuel, and other species

$$m_{fuel}(1\text{-}Xk) = D\rho(\partial Xk/\partial y) \quad (3)$$

$$m_{fuel}Xk = D\rho(\partial Xk/\partial y) \quad (4)$$

respectively. Here, m_{fuel} represents mass ejection rate of fuel, D is the diffusion coefficient, X_k are mole fractions of species, **p** is the gas density, and y is the distance from the solid surface. The surface temperature, T_W, is calculated from **an** energy balance across the burner, which is given by

$$h_w(T_w-T_{amb})=\lambda(\partial T/\partial y) \quad (5)$$

where, h_W is the heat transfer coefficient for the burner, λ is thermal conductivity, T_{amb} is the ambient temperature (298.16 K), and T_w varies along the surface, x.

In the simulations, m_{fuel} (9.0 gm/m²sec) and h, (70.0 W/m²K) are fixed and uniform along the porous surface. T_w and X_k are calculated **as** functions of x along the solid surface from equations **(3)** to (5) at each time step. Equations **(3)** to (5) are solved by fixed point iterative method at each time step for the integration of the Navier-Stokes equations.

DISCUSSION

Solutions of Navier-Stokes equations describe temperature, heat release rate, axial and vertical velocities, density, and concentrations of fuel, oxygen, carbon dioxide, water vapor, and liquid water as functions of x , y, and time, t. First, we will discuss the steady-state results for the base case (without suppressant) and make comparisons with the porous plate burner data.

Figure 1 shows temperature contours (shaded) and a single heat release rate contour (100.0 KW/m³, dark line) at steady state. The ordinate and abscissa show distance from the solid surface, y, and distance along the surface, x, respectively. Air flows from left to right and n-pentane is injected through the porous plate, which lies between x = 2.5 cm to x = 6.8 cm. The combustion reaction occurs mostly within the region confined by the heat release rate contour. At a fixed value of x, the gas temperature increases with y and reaches a maximum inside the heat release rate contour followed by a decrease to ambient temperature in the bulk air. In Figure 2, the temperature profiles at different values of x **(3** and *5* cm) are plotted together with the experimental measurements of Ramachandra and Raghunandan [8] for the porous plate burner. The theoretical predictions of maximum temperature are in excellent agreement with the data. The theory, however, appears to underpredict the flame to surface distance, which is indicated by the position of peak temperature with respect to the surface, by 20% (by less than *2* mm). The 20% discrepancy may be due to differences in the heat **loss** through the burner between the theory and experiments. **In** the experiments, the value of h_w is unknown due to the lack of detailed information regarding the burner design, which determines the heat **loss** from the surface into the burner. Figure 3 compares the predictions of axial velocity profiles with the experimental data. Clearly, the theory is in good agreement with the data. There has been some confusion regarding the exact cause for the presence of a maximum in the axial velocity profile [8]. Our model shows that the maximum in axial velocity profile occurs mainly due to the expansion effect near the leading edge, where the heat release rates are very high. The density change due to increased temperature causes the vertical mass flow to increase and axial mass flow to decrease near the leading edge. The increased vertical mass flow leads to the presence of a maximum **in** axial velocity profile at distances far from the leading edge.

The transient solutions of the Navier-Stokes equations for temperature and heat release rate contours are shown in Figure **4** at the end of the ignition period (20 msec). These solutions were obtained with fixed surface temperature, for ethane injection (0.25 cm/sec), **and** for air velocity of 30.0 cm/sec. Adiabatic boundary condition was applied **on** the leading plate **(x** = 0 to 5 cm). The porous plate (x = *5* to 10 cm) and the non-porous trailing plate (x = 10 to 18 cm) were set at ambient temperature (298.1*6* K). The solutions were obtained for dry air, air with 20 weight% steam (or 15.5 mole% O_2), and air with 20 wt.% water droplets. Ignition was achieved in all three cases **as** indicated by the dark solid line representing release of heat (100.0 KW/m³ contour) due to combustion.

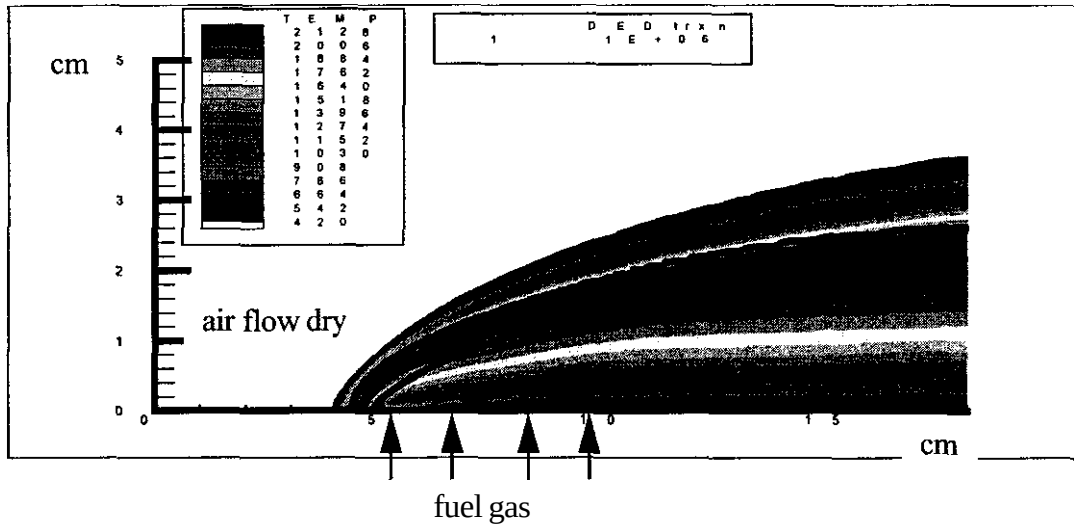

Figure 1. Temperature and heat release rate contours without the suppressants.

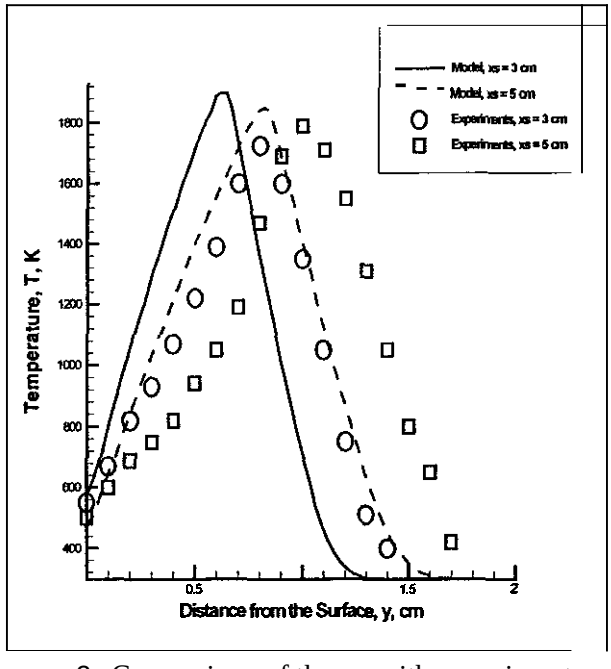

gure 2. Comparison of theory with experiment data for temperature profiles without th suppressants.

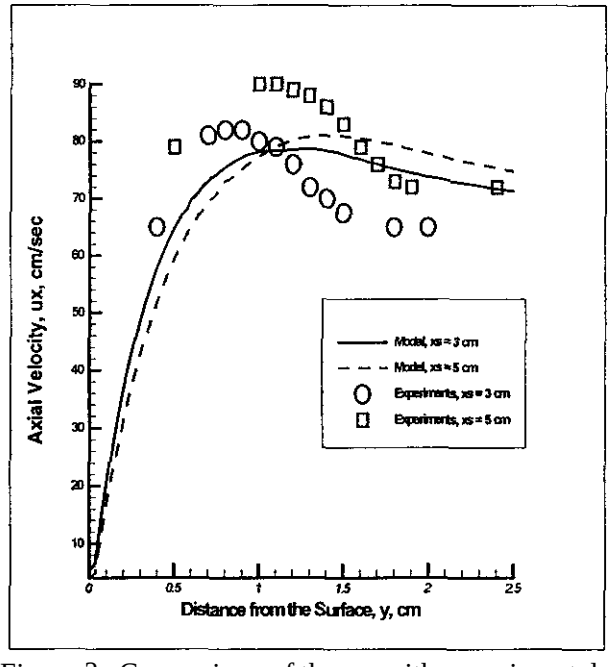

Figure 3. Comparison of theory with experimental data for velocity profiles without the suppressants.

Figure 5 shows flame spread across the porous plate in all three cases. The temperatures are lowered by about 250 K due to the effects of oxygen dilution and high specific heat (specific heat of water vapor is higher than that of air) when steam was added to the air. Water droplets lower the gas temperatures significantly due to the additional effect of the latent heat, when compared to the steam case. In the cases of dry air and steam, the heat release rate contour is anchored at the adiabatic leading plate. In contrast, in the case of water droplets, the heat release rate contour detaches from the surface forming a pocket of hot gases above the plate. Thus, the latent heat absorption seems to destabilize the flame near the leading edge. Figure 6 shows that the flames continue to spread along the surface at 420 msec. The gas temperatures at 420 msec are lower than those at 170 msec (Figure 5) in the cases of steam and water droplets. In the case of water droplets, the heat release rate contour completely clears the porous plate as the reaction

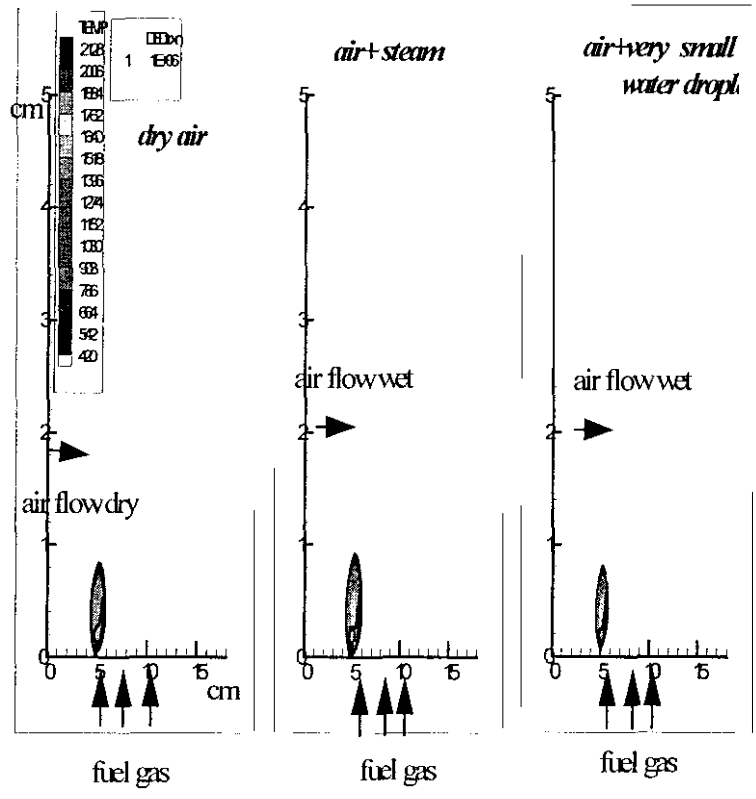

Figure 4. Temperature and heat release rate contours with and without the suppressants at 20 msec.

pocket is transported to the non-porous trailing section. Despite continued ejection of the fuel gas from the porous section (5 cm to 10 cm), no flame is formed above it. As time progresses, at 670 msec, the flame spreads across the entire plate and the heat release rate contours open up in the cases of dry air and steam as shown in Figure 7. The flame with water droplets does not appear to attach anywhere on the surface, which is at ambient temperature as indicated by the heat release rate contour. The gas temperatures continue to drop in the case of steam and water droplets. At 1420 msec, Figure 8 shows that the flame with water droplets is blown off the surface, and the reaction pocket is transported out of the computational domain leaving behind air and fuel mixture at ambient temperature. Thus, the flame intrinsically time dependent with no non-trivial steady state in the presence of the droplets. In the cases of dry air and steam, temperatures reach steady states, and addition of steam suppresses the temperature by as much as 350 K. A comparison of temperature profiles between the dry air and steam cases shows that the suppression in temperature is higher near the leading edge of the heat release rate contour than in the downstream section.

CONCLUSIONS

New solutions of full Navier-Stokes equations were obtained using Barely Implicit Flux Corrected Transport (BIC-FCT) algorithms to describe the effects of oxygen dilution, specific heat, and latent heat absorption in a boundary layer diffusion flame. The degree of suppression in temperature, due to the addition of steam and water droplets prior to ignition, appears to increase with time during the development of flame from ignition to extinction (or steady state) over the porous plate. Furthermore, the degree of suppression seems to be greater near the leading edge, which is adiabatic, than in the downstream section, which is kept at ambient temperature. The additional effect of latent heat absorption seems to destabilize the flame near the leading edge causing flame detachment from the surface in the presence of water droplets. After the detachment, the flame is transported downstream and is blown off the plate despite continued ejection of the fuel from the porous section. The steady-state solutions for the case of dry air are in good agreement with the existing experimental data for temperature and axial velocity profiles.

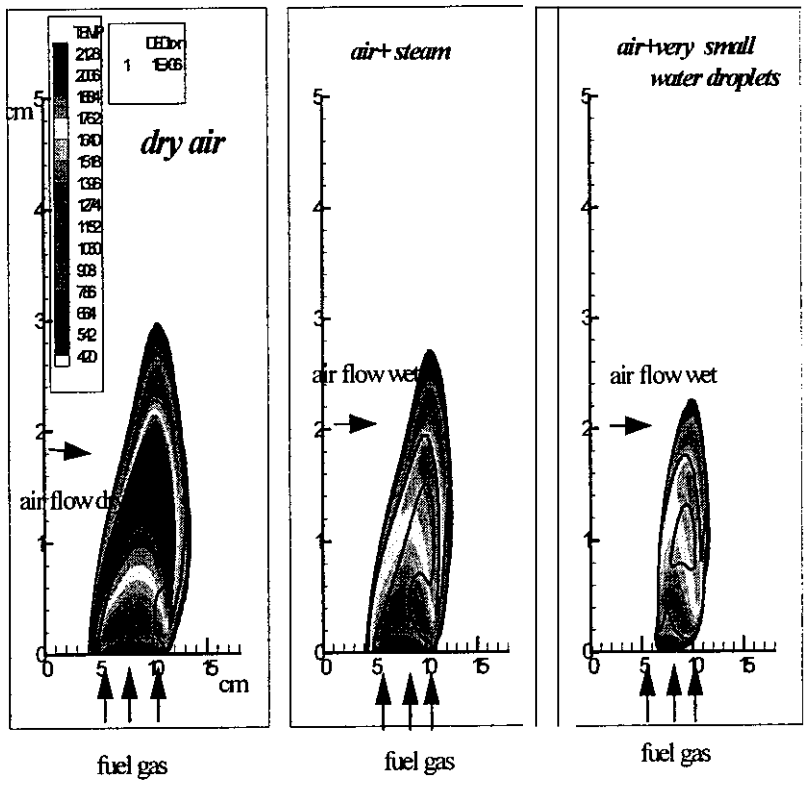

Figure 5. Temperature and heat release rate contours with and without the suppressants at 170 msec.

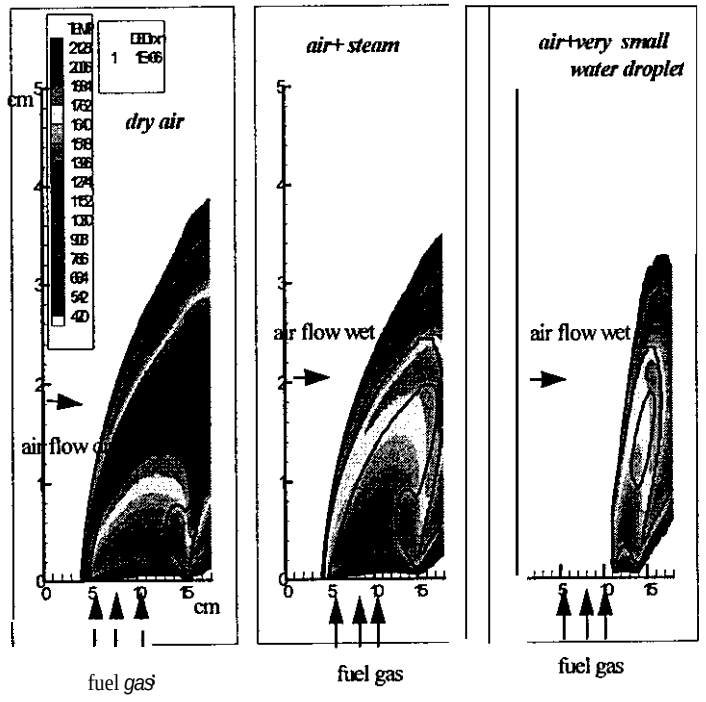

Figure 6. Temperature and heat release rate contours with and without the suppressants at 420 msec.

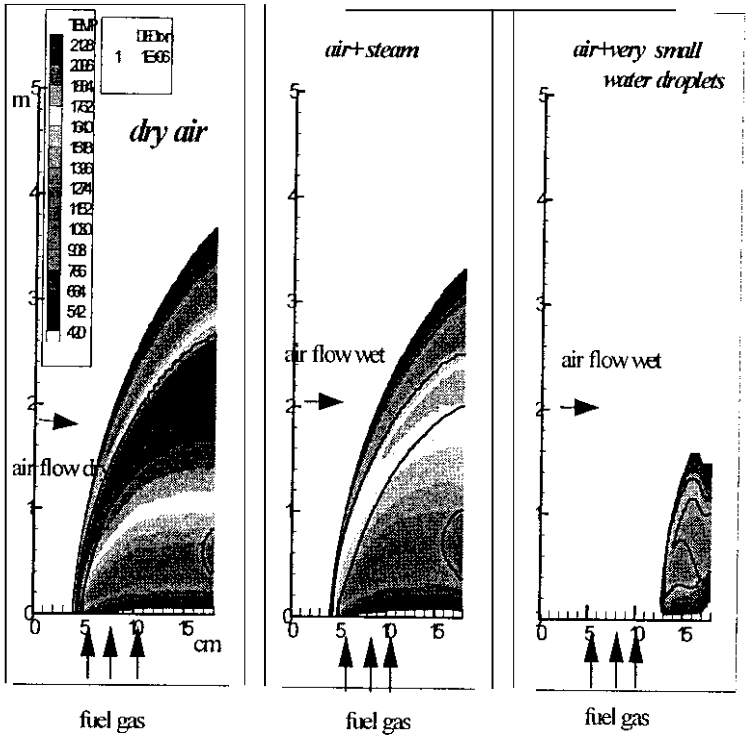

Figure 7. Temperature and heat release rate contours with and without the suppressants at **670** msec.

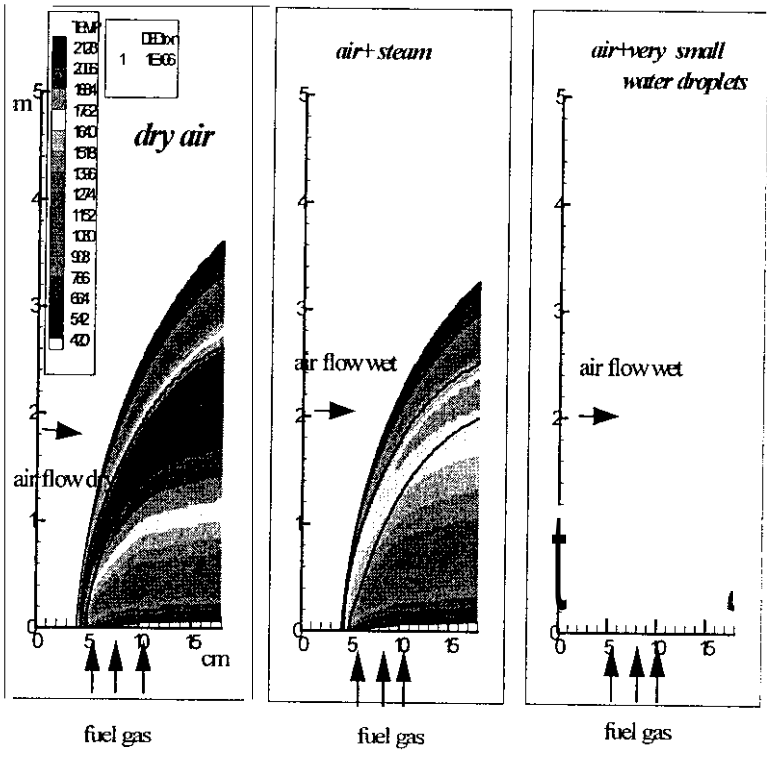

Figure **8.** Temperature and heat release rate contours with **and** without the suppressants at 1420 msec.

ACKNOWLEDGMENTS

This work was funded by the Office of Naval Research, Code **334,** under the Damage Control Task of FYOl Surface Ship Hull, Mechanical, and Electrical Technology Program (PE0602121N).

REFERENCES

1. Tatem, P.A., Beyler, C.L., DiNenno, P.J., Budnick, E.K., Back, G.G., and Younis, S.E., "A Review of Water Mist Technology for Fire Suppression," Memo Report# NRL/MR/ **6180-94 7624,** Naval Research Laboratory, Washington, DC, 1994.
2. Mawhinney, J., DiNenno, P.J., and Williams, F.W., ***Water Mist Flashover Suppression and Boundary Cooling System for Integration with DC-ARM: Summary of Testing,*** NRL Letter Report .#6180/0001, Naval Research Laboratory, Washington, DC, **1999.**
3. Prasad, K., Li, C., Kailasanath, K., Ndubizu, C.C., Ananth, R., and Tatem, P.A., "Numerical Modeling of Water Mist Suppression of Methane-air Diffusion Flames," ***Comb. Sci. & Tech.,*** 132, **325, 1998.**
4. Prasad, K., Li, C., Kailasanath, K., Ndubizu, C.C., Ananth, R., and Tatem, P.A., "Numerical Modeling of Water Mist Suppression of Methanol Liquid Pool Diffusion Flame," ***Combustion Theory & Modeling,*** **3,656, 1999.**
5. Lentati, A.M., and Chelliah, H.K., "The Dynamics of Water Droplets in Counterflow Field and Its Effects on Flame Extinction," ***Combustion and Flame,*** 115, pp. **158-179, 1998.**
6. Hirano, T., and Kanno, Y., "Aerodynamic and Thermal Structures of the Laminar Boundary Layer Over a Flat Plate with a Diffusion Flame," ***Fourteenth Symp. (International)*** on ***Combustion,*** The Combustion Institute, Pittsburgh, PA, **391, 1973.**
7. Kikkawa, **S.,** and Yoshikawa, K., "Theoretical Investigation on Laminar Boundary Layer with Combustion on a Flat Plate," ***Int. Heat Mass Transfer,*** **16, 1215, 1973.**
8. Ramachandra, **A.,** and Raghunandan, B.N., "An Analysis of a Boundary Layer Diffusion Flame Over a Porous Flat Plate in a Confined Flow," ***Combust. Sci. and Tech.,*** 38, 59, **1984.**
9. Mao, C.-P., Kodama, H., and Fernandez-Pello, A.C., "Convective Structure of a Diffusion Flame Over a Flat Combustible Surface," ***Combustion and Flame,*** **57,209, 1984.**
10. Kodama, **H.,** Miyasaka, K., and Fernandez-Pello, A.C., "Extinction and Stabilization of a Diffusion Flame on a Flat Combustible Surface with Emphasis on Thermal Controlling Mechanisms," ***Combust. Sci. and Tech.,*** 54, 37, **1987.**
11. Chen, C-H., and Tien, J., "Diffusion Flame Stabilized at the Leading Edge of a Fuel Plate," ***Comb. Sci. and Tech.,*** **50,283, 1986.**
12. Di Blasi, C., "Modeling and Simulation of Combustion Processes of Charring and Non-charring Solid Fuels," ***Prog. Energy Combust. Sci.,*** 19, 71, **1993.**
13. Patnaik, G., Laskey, K.J., Kailasanath, K., Oran, E.S., and Brun, T.A., ***FLIC-A Detailed, Two Dimensional Flame Model,*** NRL Memorandum Report **6555,** Naval Research Laboratory, Washington, DC, September **1989.**
14. Westbrook, C.K., **and** Dryer, F.L., "Chemical Kinetic Modeling of Hydrocarbon Combustion," ***Prog. Energy Combust. Sci.,*** **10,** 1, **1984.**